REPORT

APCC Young Scientist Support Program 2016

Predictability of oceanic and atmospheric indices in global models for seasonal forecast in Chile

José Vicencio Veloso

APCC Counterpart: Dr. Vladimir Kryjov

1. INTRODUCTION

The seasonal variability of precipitation and temperature has strong impact on both economic and social aspects in Chile. Long periods of dry or wet weather, several weeks with high temperatures or strong colds waves, directly affects the population and most of the economic activities.

In recent years, unusual weather events have occurred in most regions of the country. Since 2007, a strong and continuous drought had resulted to a decrease in farm production in the north and central part of the country; also generating a significant decrease in the amount of water reservoirs in lakes, rivers and dams; adding to an enormous pressure in the power electricity production.

In the south of the country, warm and dry summers had been observed, affecting agriculture, animal breeding and forest industry. According to the data of National Corporation of Forest (CONAF), there was a registered increase in forest fires in the previous years, associated with higher burnt areas. Uncontrolled forest fires did not only affect forest plantation, but also national parks and cities.

The variability of the rainfall and precipitation has been study by several authors (Aceituno, 1998; Aceituno and Montecinos, 1993; Garreaud and Rutllant, 1996; Rutllant, 1987; Rutllant and Fuenzalida, 1991; Montecinos and Aceituno, 2003). These studies suggest the strong dependency between ENSO (El Niño-Southern Oscillation) and the change in seasonal rainfall, also in temperature, due to the Pacific South America Teleconnection (Mo and Higgins, 1998). In recent years, other studies (Quintana and Aceituno, 2011) suggest the strong influence of the atmospheric patterns in the South East Pacific, such as the Regional Antarctic Oscillation and South East Pacific High, in the annual variability of precipitation. However, there are no studies conducted that had related the influence of these two patterns to temperature, with a time scale lower than a year, such as monthly or seasonal.

The first objective of this research is to determine the relationship between the oceanic and atmospheric indices, to the quarterly precipitation, and the maximum and minimum temperature in Chile for the period of 1971-2014. To fill the gap in the understanding of the

behavior of these three meteorological parameters, more than thirty stations were used distributed throughout the country.

The second goal is to determine the ability of the selected global models to predict atmospheric and oceanic index. This would enable us to select the best indexes to use in the implementation of the new seasonal forecast.

The third and final objective is to calculate the skill of the forecasted index to predict precipitation and temperature. This point will give us the opportunity to improve the seasonal forecast using global model data.

2. DATA AND METHODS

2.1. DATA

The weather stations used to this study are selected (see Figure 1) which aims to cover most of the regions in country. There are 33 surface stations in total. The data was obtained from the Dirección Meteorológica de Chile (DMC), Dirección General de Aguas (DGA), Climate and Resilience Center (CR2) and Armada de Chile (ACH). The surface stations used are shown in Table 1.

The monthly El Niño indices were obtained from NOAA – ESRL (National Oceanic and Atmospheric Administration-Earth System Research Laboratory) webpage (http://www.esrl.noaa.gov/psd/gcos_wgsp/Timeseries) from HadlSST1 dataset (*Rayner et all, 2003*).

There are three atmospheric indices representing the South East Pacific variability of the sea surface pressure. The first index corresponds to the South East Pacific Subtropical High (SEP-High), which was constructed using the first principal component of the average pressure in eight stations in Continental Chile and Eastern Island, as can be seen in Figure 2, surrounding the climatological position of the Subtropical High Pressure system. This index represents the intensity of the Subtropical High (*Quintana and Aceituno, 2011*). The index was computed with the station pressure data information from DMC.

The positive (negative) values of the index correspond to a stronger (weaker) than normal subtropical anticyclone.

The second index corresponds to the pressure difference in two regions of the South East Pacific, called the South East Pacific Antarctic Oscillation (SEP-AAO). This index is the meridional difference of sea level pressure, constructed using the data from NCEP-NCAR (National Centers for Environmental Prediction-National Center for Atmospheric Research) Reanalysis (*Quintana and Aceituno, 2012*).

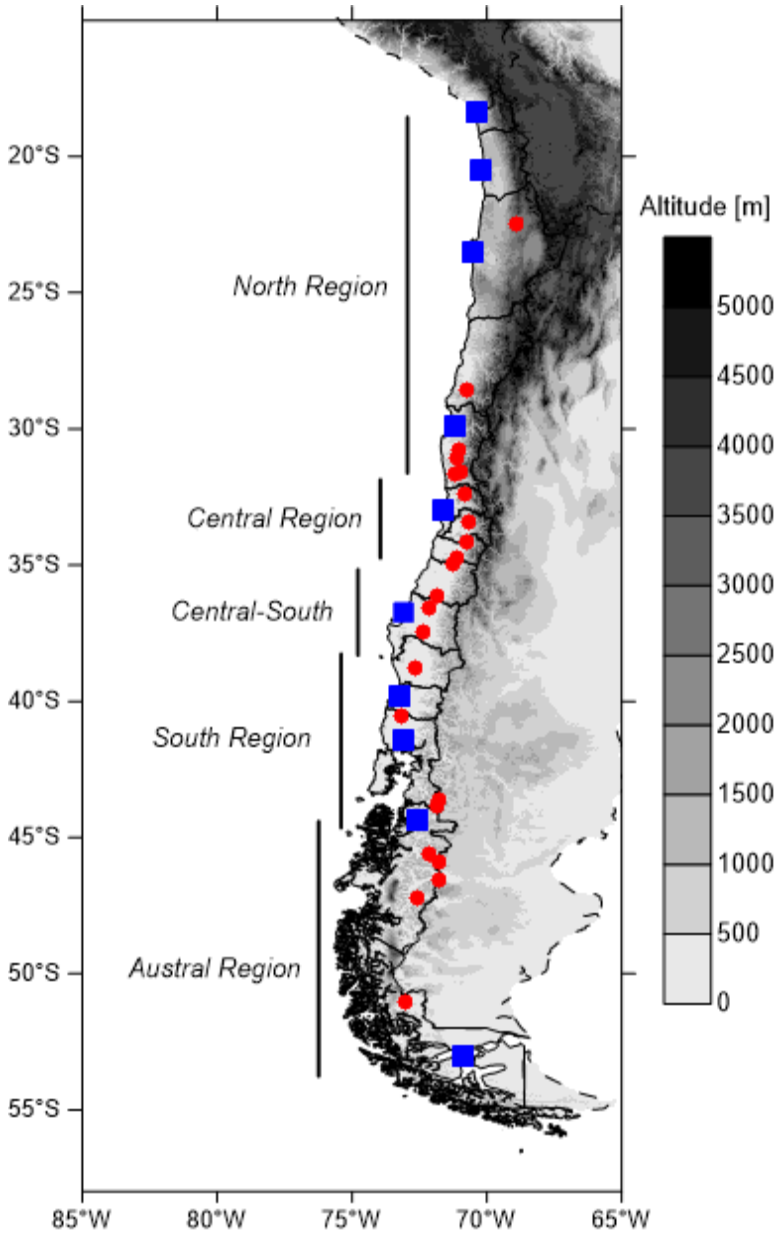

Figure 1. Distribution map of surface stations used in this study. The stations located in the coast are represented by a blue square and the inland/valley stations are represented by a red circle. The map also shows the names of the principal macro-regions in the country and the terrain altitude in meters.

Table 1. Latitude, longitude and localization (coastal or inland) of the stations used. For Data type, TX corresponds to maximum temperature, TN for minimum temperature and RR for precipitation. Data obtained from DGA is marked with an asterisk (*) and ACH data is marked with two asterisks (**).

Station Name	Latitude (°S)	Longitude (°W)	Location	Data type
Arica	-18.40	-70.40	Coastal	TX and TN
Iquique	-20.50	-70.20	Coastal	TX and TN
Calama	-23.50	-68.90	Inland	RR, TX and TN
Antofagasta	-22.50	-70.50	Coastal	TX and TN
Vallenar*	-28.60	-70.76	Inland	RR, TX and TN
La Serena	-29.90	-71.20	Coastal	RR, TX and TN
La Paloma Res.*	-30.80	-71.00	Inland	RR
Cogoti 18*	-31.10	-71.10	Inland	TX and TN
Huintil*	-31.57	-70.96	Inland	RR
Illapel*	-31.65	-71.16	Inland	RR
Alicahue*	-32.39	-70.79	Inland	RR, TX and TN
Valparaiso**	-33.01	-71.64	Coastal	RR, TX and TN
Santiago	-33.44	-70.66	Inland	RR, TX and TN
Rancagua*	-34.18	-70.77	Inland	RR
Convento Viejo*	-34.78	-71.09	Inland	RR
Curicó	-34.96	-71.25	Inland	RR, TX and TN
Parral*	-36.12	-71.84	Inland	RR
Chillán	-36.60	-72.11	Inland	RR, TX and TN
Concepción	-36.76	-73.07	Coastal	RR, TX and TN
Los Ángeles	-37.46	-72.36	Coastal	RR and TX
Temuco	-38.76	-72.64	Inland	RR, TX and TN
Valdivia	-39.79	-73.25	Coastal	RR, TX and TN
Osorno	-40.58	-73.14	Coastal	RR, TX and TN
Puerto Montt	-41.44	-73.06	Coastal	RR, TX and TN
Futaleufú	-43.82	-71.82	Inland	RR
Alto Palena	-43.61	-71.80	Inland	RR
Puerto Puyuhuapi*	-44.38	-72.57	Coastal	RR
Coyhaique	-45.61	-72.11	Inland	RR, TX and TN
Balmaceda	-45.92	-71.73	Inland	RR, TX and TN
Chile Chico	-46.57	-71.73	Inland	RR, TX and TN
Lord Cochrane	-47.26	-72.59	Inland	TX and TN
Torres del Paine*	-51.08	-73.04	Inland	TX and TN
Punta Arenas	-53.01	-70.86	Coastal	RR, TX and TN

Positive (negative) values of the index are related with higher (lower) than normal sea level pressure in the area near 60°S and lower (higher) than normal near 40°S. Positive values are usually related with high pressure blocking in the Bellingshausen sea, to the west of

Antarctic Peninsula. The figure 2 show the areas were the sea surface pressure is extracted. Negative values are related with anticyclone blocking near 40°S, west of the southern Chile.

The last index corresponds to the difference in the observed surface pressure of two meteorology stations in Chile; one located at Puerto Montt City (42°S) and the other located in the Antarctic Peninsula, the Presidente Eduardo Frei Montalva station (62°S), as can be seen in figure 2. The index was calculated using the pressure data obtained from DMC.

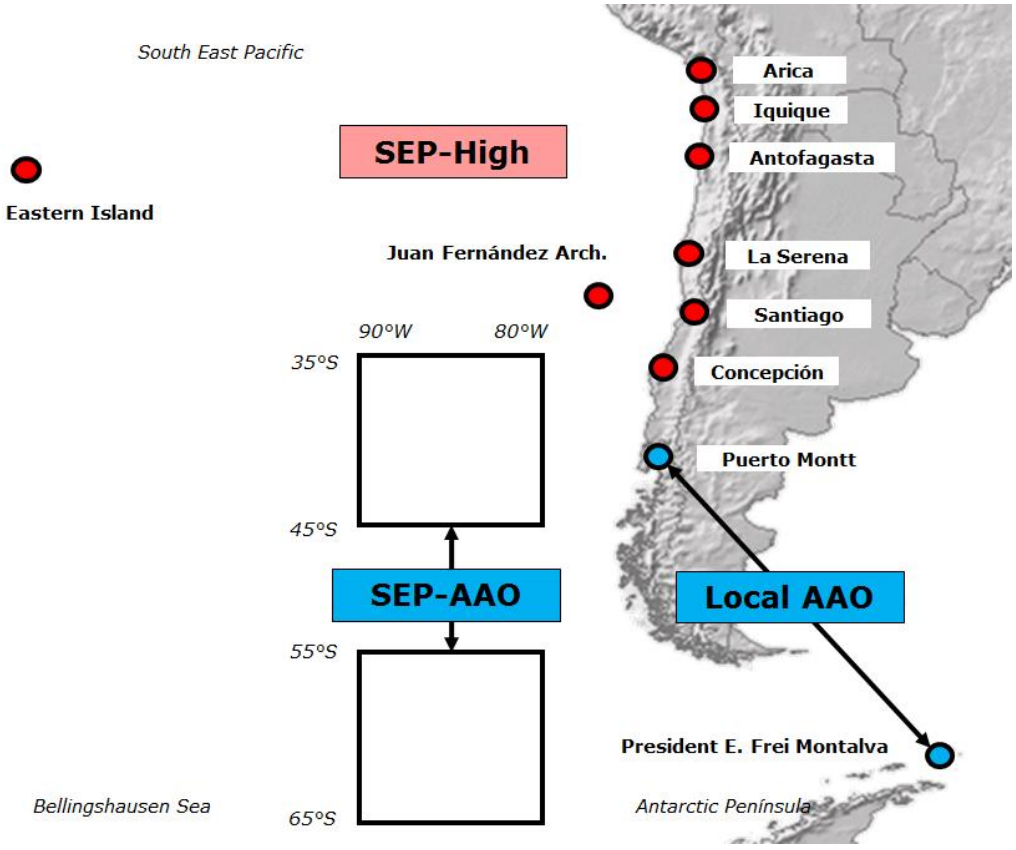

Figure 2. Schematic map of the distribution of the stations used to construct SEP-High index (red circles), Local-AAO index (blue circles) and the areas of average sea level pressure (black boxes) in South East Pacific Ocean. Is also included the name of each station.

The data used from global models were obtained from APCC HPCC (APEC Climate Center-High Performance Computer Cluster) Server. The global models used are APCC (APEC Climate Center), POAMA (Predictive Oceanic and Atmospheric Model for

Australia), NOAA, PNU (Pusan National University) and NCEP (National Center for Environmental Prediction). The data used was the hindcast of sea level pressure and sea surface temperature, with spatial resolution of 2.5°.

The observed sea surface temperature was obtained from IRI (International Research Institute) Online Library. Data correspond to the NOAA NCDC ERSST (National Climate Data Center-Extended Reconstructed Sea Surface Temperature) Version 4, with a horizontal grid resolution of 2.0°.

2.2. METHODOLOGY

The Pearson Correlation was used as the principal analysis in this study. For the first objective, the quarterly precipitation and temperature data from the 33 surface stations will be related to the quarterly data of El Niño, SEP-High and SEP-AAO indexes.

For the second objective, the quarterly sea level pressure and sea surface temperature data will be extracted from the hindcast data of the five global models. Every model has different amount of ensemble members for every quarterly hindcast data. We will use the average (mean) of ensemble members, generating five different forecast for every quarter of the year.

The construction of the indices used the same structure with the observed indexes. The forecasted indices shall be compared to the observed indexes in a time-period of 30 years (data of 1981 to 2010) to determine the skills of the different models to forecast the indices.

After this, the second set of forecasted indices will be created. This new set will correspond to a new way of information extraction from the models. The areas of sea level pressure or sea surface temperature from the models where the indices are best represented considering the highest levels of correlation, will become in the new areas where we will extract the information and create the new set of forecasted indexes.

For the final objective, the correlation level shall be calculated between the observed quarterly precipitation and temperature, and the forecasted indices, for both observed

normal and new. Later on, the observed correlation in representative stations will be compared to the forecasted indices.

3. RESULTS

3.1. OBSERVED SEASONAL VARIABILITY OF THE RAINFALL AND TEMPERATURE IN CHILE

3.1.1. PRECIPITATION AND ATMOSPHERIC INDICES

The South East Pacific Antarctic Oscillation (SEP-AAO) and the Local Antarctic Oscillation (Local AAO) indices both present moderate to high level of inverse correlation (-0.5 to -0.7). Figure 3 shows the correlation between the precipitation and SEP-AAO, where the blue gradients represent the highest inverse correlation between the index and the quarterly rainfall, noticeably concentrated in 27°S and 41°S during most of the year. The area with the highest inverse relation is located in the central-south region, approximately between 34 to 36°S at the end of the austral winter and the spring (JAS to OND).

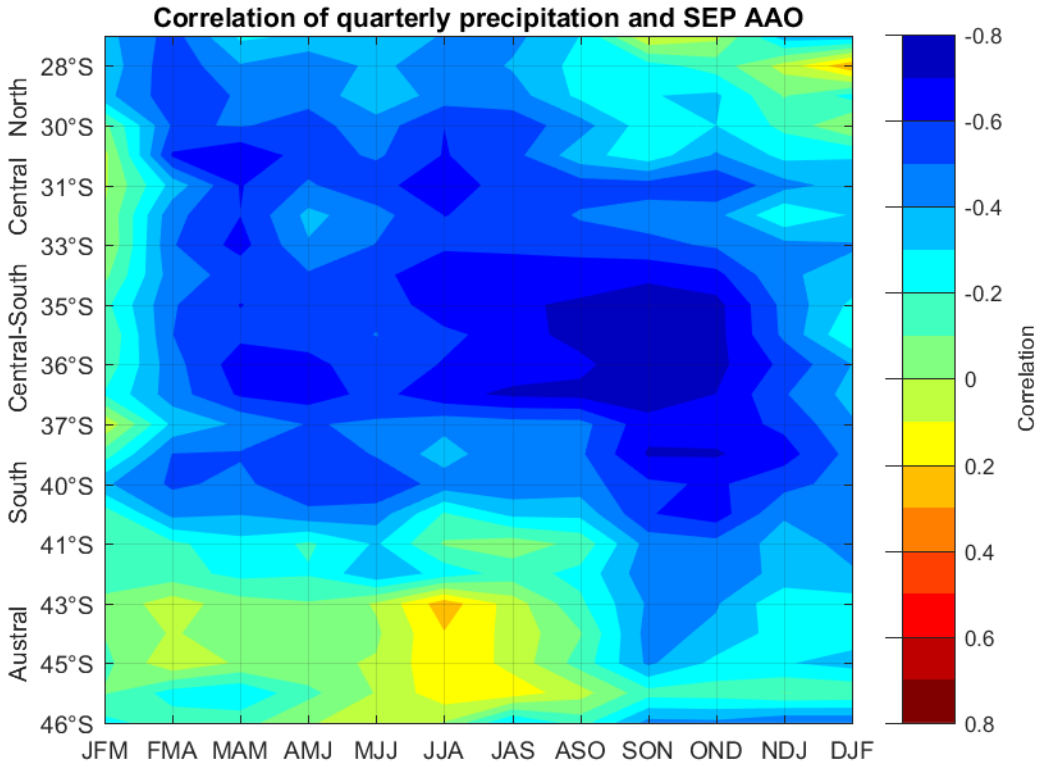

Figure 3. Correlation coefficient for quarterly precipitation and the SEP-AAO index, computed for 24 stations latitudinal distributed from north to south in the y-axis. X-axis shows the quarterly division of the year. Colors represent the level of correlation (Climate period: 1971-2014).

In the Austral region (41 to 46°S), it is not possible to find any strong linear connection between the SEP-AAO or Local AAO and rainfall, at least in the quarter perspective.

In the case of the South East Pacific Subtropical High (SEP-High), the level of inverse correlation is moderate (r = -0.5) between 27°S and 40°S, reaching the maximum values (r = -0.6) in central region between MJJ and JAS.

Meanwhile in the central region, the highest levels are concentrated in the austral winter. In the central south and south region (35 to 40°S), the highest inverse correlations are found during the fall and spring season, reaching near -0.6, decreasing toward the south, disappearing from 41°S to the 46°S (the austral region). Here again, it is not plausible to find some correlation level between the index and rainfall in any quarter of the year.

3.1.2. PRECIPITATION AND EL NIÑO INDICES

All indices show the same three patterns of correlations between the observed sea surface temperature in the four El Niño regions and the observed precipitation. The first pattern is possible to find in the north and central region (27 to 34°S). Here, the highest direct correlation (+0.4 to +0.6) is present between AMJ and ASO, coinciding with the austral winter. The correlation level is higher in El Niño 3 and 3.4, and lower in El Niño 1+2 and 4. Figure 4 shows the correlation map between El Niño 3.4 index and the quarter rainfall, where red gradients represent the highest correlation levels.

The second pattern is located in the central south and south region (34 to 40°S), where the correlation level is moderate to high (+0.4 to +0.6) during ASO and OND, and the signal is strong especially with El Niño 3 and 3.4 indices.

The last pattern corresponds to an area of negative low to moderate correlation level (-0.3 to -0.4) between DJF and JFM in the central south and south region (34 to 40°S), and extended from NDJ to FMA in the austral region. The pattern is strongest in El Niño 1+2 index.

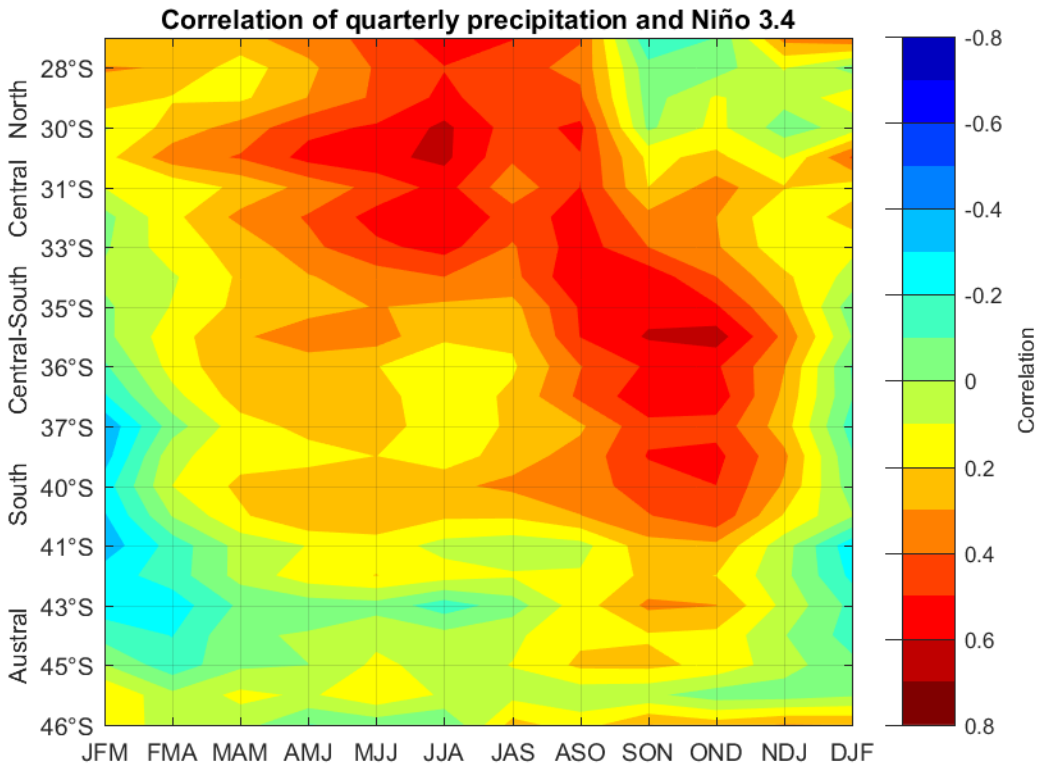

Figure 4. Correlation coefficient for quarterly precipitation and El Niño 3.4 index, computed for 24 stations latitudinal distributed from north to south in the y-axis. X-axis shows every quarter of the year. Colors represent the level of correlation (Climate period: 1971-2014).

3.1.3. MAXIMUM TEMPERATURE AND ATMOSPHERIC INDICES

For the AAO regional indices, negative correlations were found in the cities of the north, central and part of the central south regions (18°S to 37°S) in coastal areas. These correlations vary from -0.4 to -0.6 most of the year. Towards the south, the inverse linear relationship disappears, appearing a region of moderate to high positive correlation in Punta Arenas (53°S) during winter and spring.

For inland stations, moderate (-0.4 to -0.6) correlation levels were found in the central and central-south regions (33°S to 37°S) during ASO and DJF, which corresponds to the spring to summer season. In the austral region, between 43°S and 51°S, moderate to high correlations (+0.4 to +0.7) were found, concentrated during MAM and SON.

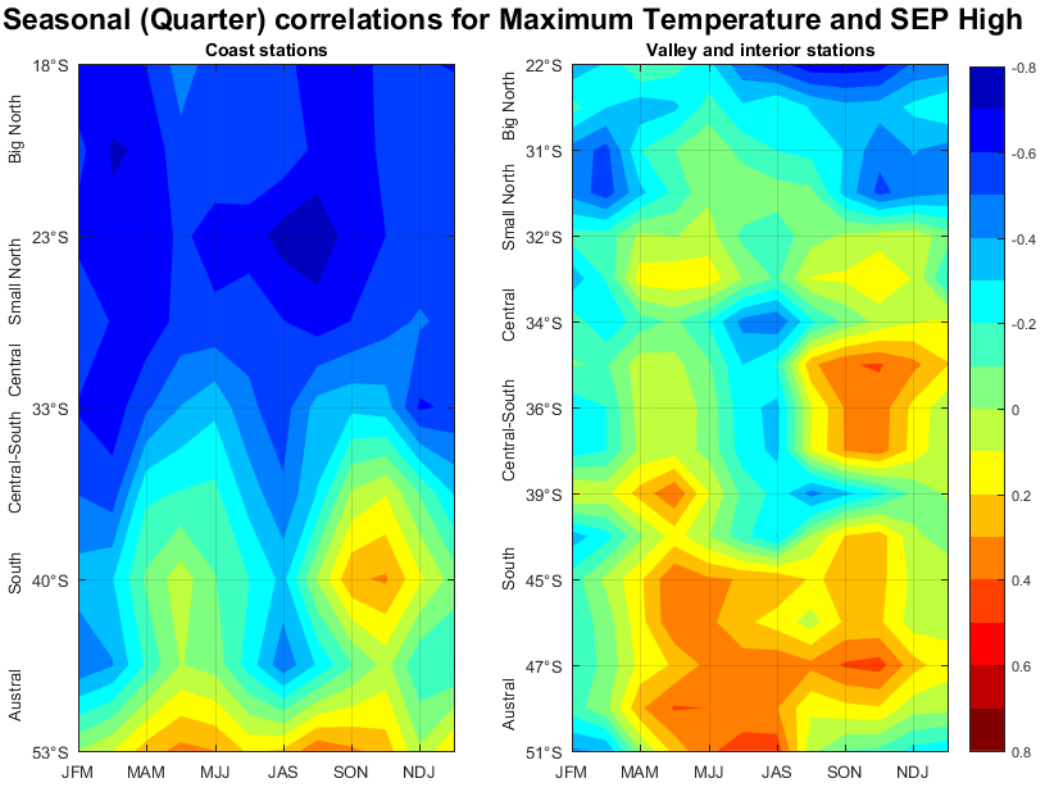

Figure 5. Correlation coefficient for quarterly maximum temperature and SEP-High index, computed for 9 coastal stations (left panel) and 17 valley stations (right panel), latitudinal distributed from north to south in the y-axis. X-axis shows every quarter of the year. The colors represent the level of correlation (Climate period: 1971-2014).

For the SEP-High index, as can be seen in Figure 5, the inverse correlation is moderate to high (-0.4 to -0.7) in the coastal stations in the north and central region (18°S to 33°S) most of the year. Toward the pole, the correlation in the coastal stations is relatively lower, with two peaks in the south region (35 to 42°S) during JFM and FMA, as well as in JJA.

In the valleys and inland stations, the pattern shows low to moderate inverse correlation in the northern stations, reaching near -0.5 during JJA to NDJ in Calama station (22°S). In the central region, however, it is only possible to identify low correlation index (+0.3 to +0.4) during SON and OND. In the Austral region, from 42°S to 51°S, the positive correlations reach low values (+0.3 to +0.4) between MAM and OND.

3.1.4. MAXIMUM TEMPERATURE AND EL NIÑO INDICES

In the valley and inland stations, it is not possible to find any level of correlations for any of the index of El Niño. The only exception is the Calama station, in the middle of the Atacama Desert (23°S), where the quarterly maximum temperature is good modulated (r = +0.6) in El Niño 1+2, 3, 3.4 and 4.

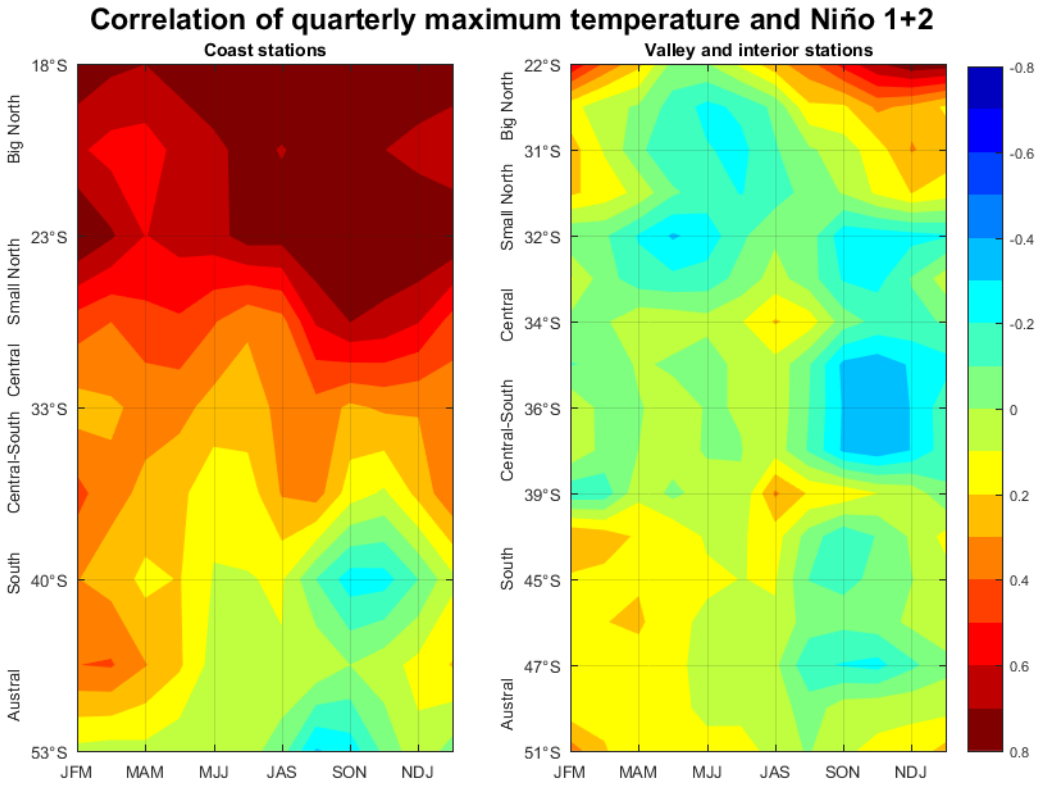

Figure 6. Correlation coefficient for quarterly maximum temperature and El Niño 1+2 index, computed for 9 coastal stations (left panel) and 17 valley stations (right panel), latitudinal distributed from north to south in the y-axis. X-axis shows every quarter of the year. The colors represent the level of correlation (Climate period: 1971-2014).

For the coastal stations, the situation is different. As shown in Figure 6, the correlation level in the northern stations for all El Niño index are very high (+0.6 to +0.8) for most of the year, especially strong during El Niño 1+2.

The dark red contour is spread out on most of the quarters and the stations in the northern coast. In the central and central south region, the correlation level is low to moderate (+0.3

to +0.5) most of the year. In the southern of the country (35 to 42°S), the highest correlation levels were attained in JFM to MAM periods.

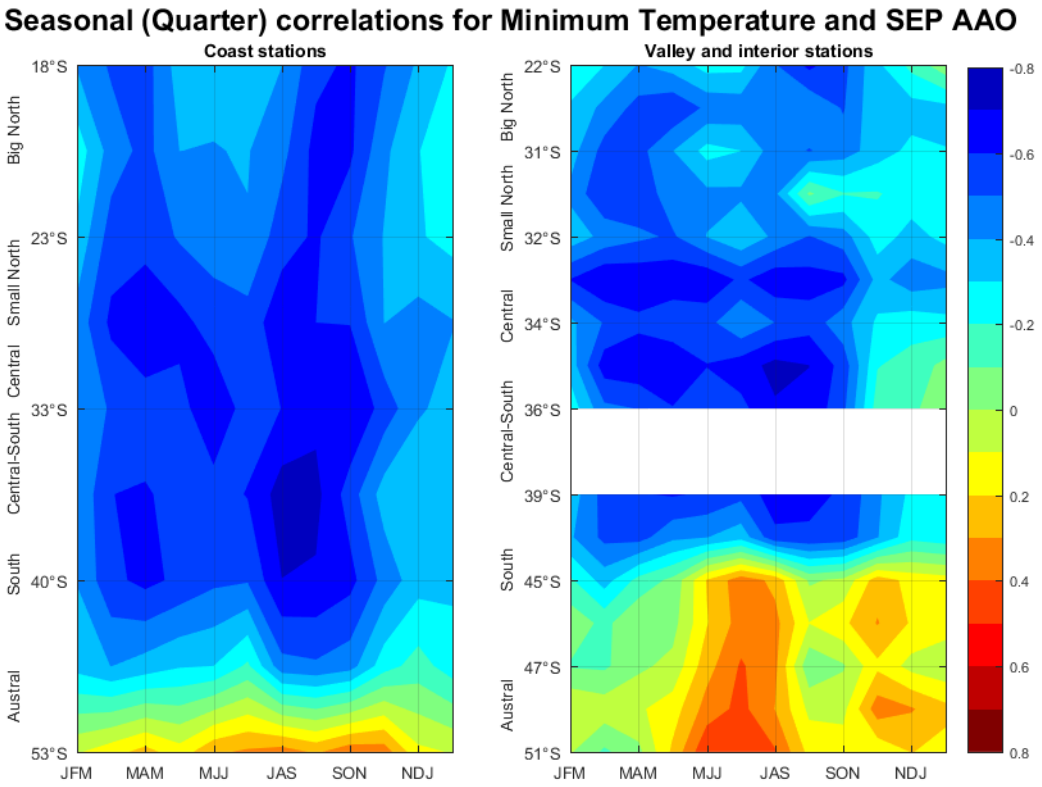

Figure 7. Correlation coefficient for quarterly minimum temperature and SEP-AAO index, computed for 9 coastal stations (left panel) and 17 valley stations (right panel), latitudinal distributed from north to south in the y-axis. X-axis shows every quarter of the year. The colors represent the level of correlation (Climate period: 1971-2014). Blank area in the right panel is due to the absence of data in Los Angeles station.

3.1.5. MINIMUM TEMPERATURE AND ATMOSPHERIC INDEXES

For the regional indices, the Antarctic Oscillation (both SEP-AAO and Local AAO) is well defined in an area of moderate to high inverse correlation (-0.4 to -0.7) during most part of the year; both for coastal and valley stations from 18°S to near 42°S. As shown in Figure 7, the dark blue areas in the south region of the coastal stations represent a correlation level of near -0.7 during the JAS and ASO period (left panel). In the valley stations, the correlations also reach near -0.7 in the area near the central south region.

The SEP-High index shows moderate to high correlation level for minimum temperature for most of the quarters of the year; both for coastal and valley stations between north to south region (18 to 42°S). The highest correlation reach near -0.8 during the austral winter, especially between 22°S to 40°S from JJA to SON. The austral region shows very weak positive correlation especially during MJJ to JAS. Nevertheless, the correlation values would not impose statistical significance.

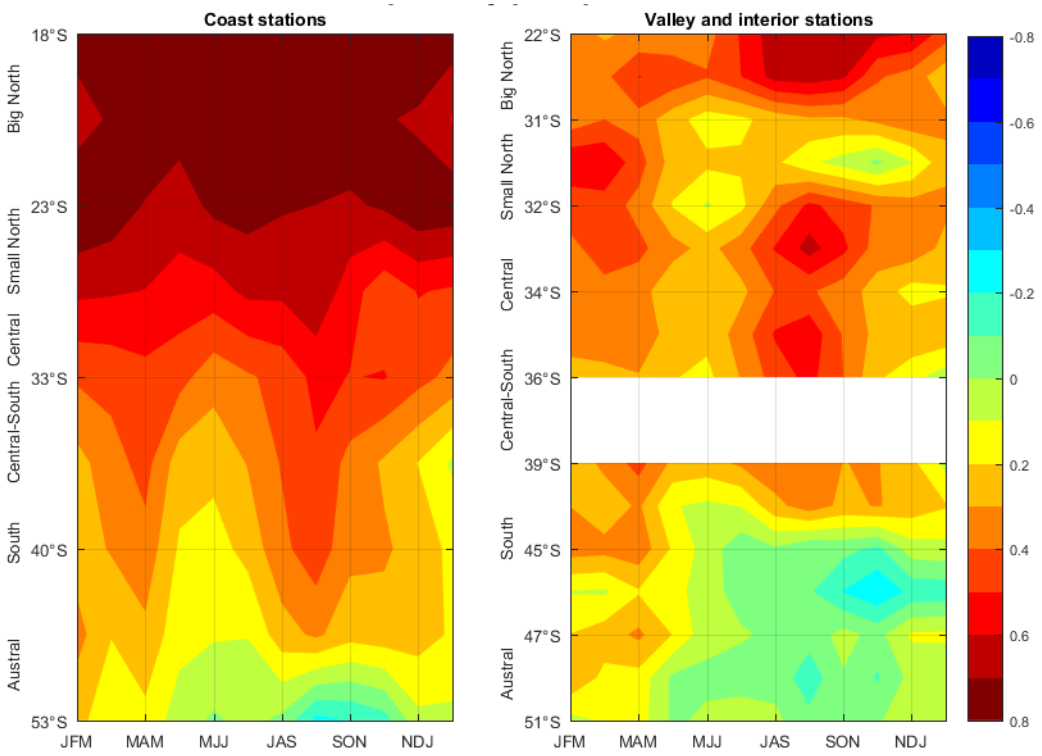

Figure 8. Correlation coefficient for quarterly minimum temperature and El Niño 3 index, computed for 9 coastal stations (left panel) and 17 valley stations (right panel), latitudinal distributed from north to south in the y-axis. X-axis shows every quarter of the year. The colors represent the level of correlation (Climate period: 1971-2014). Blank area in the right panel is due to the absence of data in Los Angeles station.

3.1.6. MINIMUM TEMPERATURE AND EL NIÑO INDICES

The stations located in the coast of the country present high correlation levels (+0.6 to +0.8) during most of the quarters of the year. This high level of correlation was found in each of oceanic index, especially in El Niño 1+2 and El Niño 3. This can be observed in Figure 8

(left panel), where the dark red color is spread out in most of the coastal and northern stations.

Arica (18°S), Iquique (20°S) and Antofagasta (23°S) stations shows the most important correlation levels in linear relation, reaching a maximum correlation value near +0.85 in some of the quarters.

Toward the central, central south and south regions, the correlation levels start to weaken with values oscillating between +0.4 to +0.6, especially in El Niño 3, 3.4 and 4 from 35 to 42°S.

In the case of valley and inland stations (Figure 8-right panel), the moderate correlations are present in most of the north, central, central-south and south stations, with values between +0.3 to +0.5, especially in El Niño 3, 3.4 and 4.

3.2. PREDICTABILITY OF THE ATMOSPHERIC AND OCEANIC INDICES USING GLOBAL CLIMATE MODELS

3.2.1. SEP-HIGH INDEX

The analysis shows that, in general, a moderate level of SEP-High index predictability result from the majority of the global models used. The quarterly averages signifies differences, where the highest correlations can be found in the quarters JAS and ASO (r = +0.66). Less predictability is found in the time periods of NDE and DEF, reaching a *r* of +0.42.

Among different quarters, there is no observed difference. An important dispersion was observed in the performance of the five climate models. As seen in Figure 9, some models tend to reach higher predictability levels compared to others. For one, APCC model achieves low and non-significance statistical correlation level, especially during EFM. However, at the same quarter, NASA model reach the highest correlation level (r = +0.8) among all models.

If the analysis is made for annual terms, the best models are found to be NASA and NCEP, reaching both higher level of Subtropical High predictability, with Pearson correlation of

+0.68 and +0.53, respectively. Lower levels of predictability are found with PNU, APCC and POAMA models, with +0.48, +0.49 and +0.51 correlation, respectively.

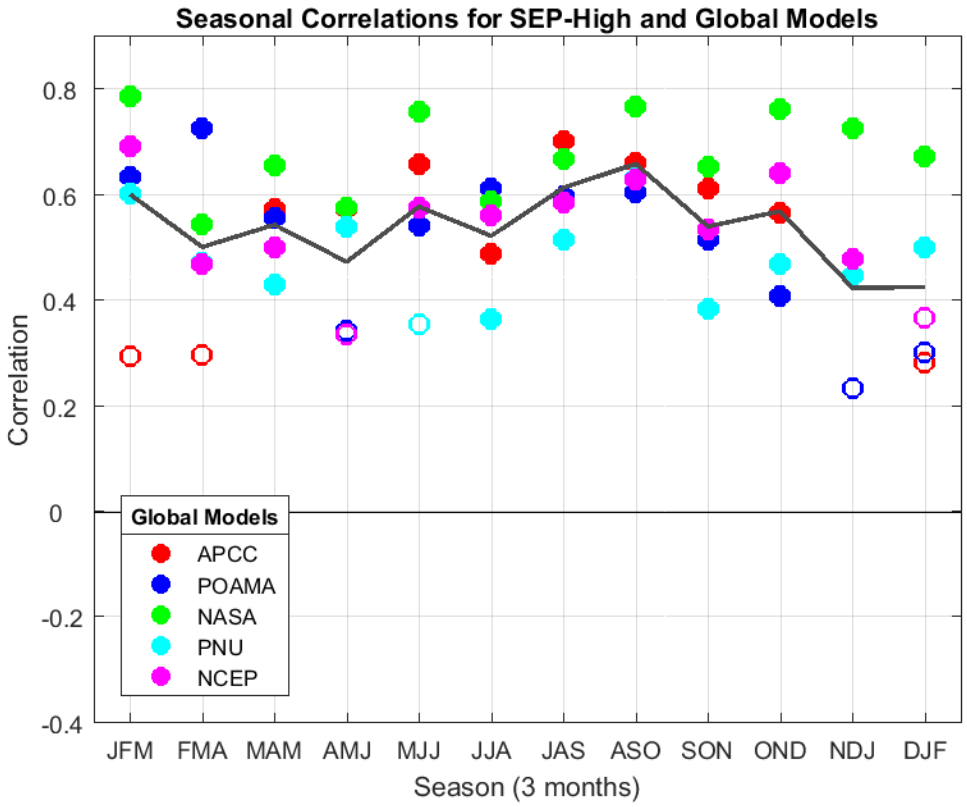

Figure 9. Correlation coefficient for the observed and forecasted SEP-High index, considering five different models (represented in different colored circles). X-axis represents the quarters of the year. Filled markers represent 95% or more statistical significance. The gray line corresponds to the average of the five models for every quarter.

3.2.2. SEP-AAO index

For the case of the SEP-AAO index, the dispersion of the correlation levels per quarter is higher than the previous SEP-High index. In Figure 10, the correlation decay in all models can be determined (gray line) during the austral winter period, where the lowest predictability values are observed during JJA (Pearson correlation of +0.31).

The higher correlations are found near FMA and OND, gaining a correlation of +0.6, with a peak of +0.63, similar to the average of all models in OND.

In annual terms, the POAMA model achieve the best performance (r = +0.59), where the best predictability quarter (r = +0.8) was observed during FMA. The least performance, however, was demonstrated by APCC model, with an annual average of +0.41 with many quarters recording no statistical significance correlation level, as shown as unfilled markers in Figure 9 (EFM, MAM, JJA and DEF).

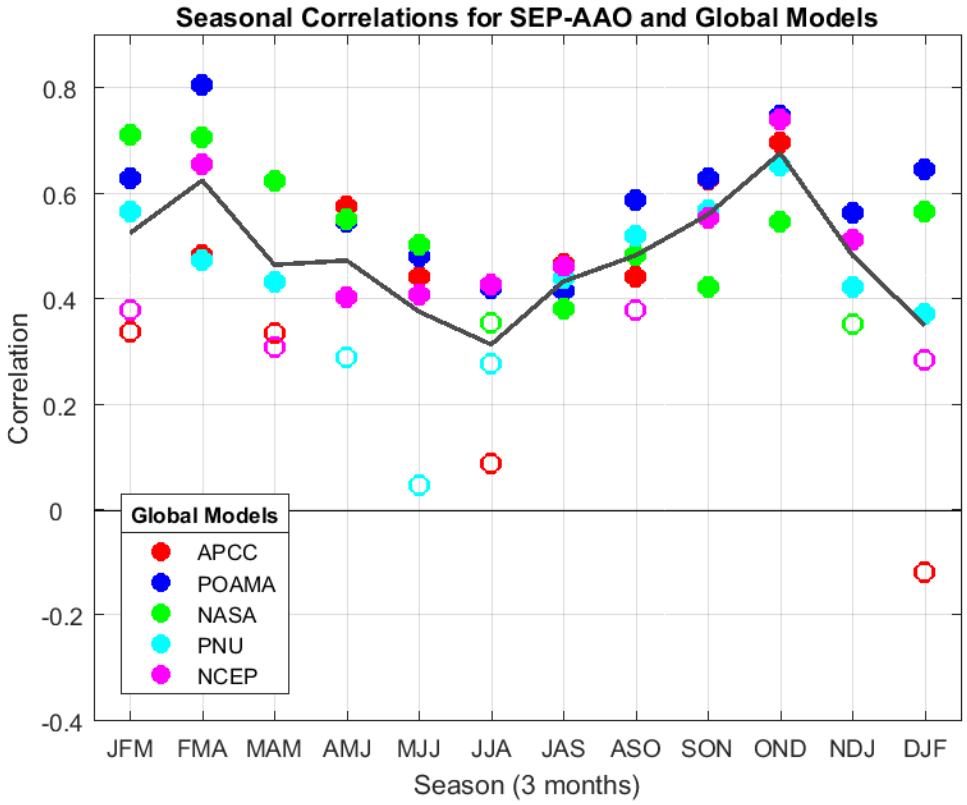

Figure 10. Correlation coefficient for the observed and forecasted SEP-AAO index, considering five different models (represented in different colored circles). X-axis represents the quarters of the year. Filled markers represent a 95% or more statistical significance. The gray line corresponds to the average of the five models for every quarter.

3.2.3. Local AAO Index

The local AAO index has one of the lowest predictability levels, bordering an annual correlation average of +0.22 for all models. The quarterly average of the five models shows that correlation levels are low most of the year. The best time period is present in OND and AMJ, with correlations of +0.42 and +0.36, respectively.

Significant differences were observed between each global model. The annual average is lower with NASA model, followed by PNU and APCC models, with correlations levels of +0.08, +0.15 and +0.24, respectively. These models did not reach a statistical significance of 95% for most of the quarters of the year. Higher predictability was found, however, with POAMA model with an annual correlation average of +0.36.

3.2.4. El Niño Indices

Results show very high predictability of El Niño 4, 3.4 and 3 in most of the models used in this study, presenting a correlation level of over +0.8 in most of the quarters. Highest correlation levels are attained during ASO and FMA, reaching +0.95, +0.97 and +0.96 during JFM for the model averages for El Niño 4, 3.4 and 3, respectively. The time period with lower correlation was found around AMJ and JAS, with an average correlation of +0.83 for El Niño 4 and +0.85 for El Niño 3.4 and 3 for MJJ.

The observed differences between each model are relatively small. The annual correlation average is consistently higher with POAMA and NASA models, reaching +0.94 and +0.93 for El Niño 4 and 3.4, and +0.97 and +0.96 for El Niño 3. The lowest correlations levels are found with PNU and NCEP models, with an approximate average of +0.85 for El Niño 4 and 3.4, and +0.87 for El Niño 3.

For the case of El Niño 1+2 index, the predictability is less high compared to the previous El Niño indices. As seen in Figure 11, most of the correlation levels fall between +0.7 and +0.9 for most of the quarters of the year. The predictability is higher during JJA and DJF, with correlations levels around +0.88 for the average of the five models. The predictability is lower between MAM and AMJ, with an average correlation of +0.77.

In Figure 11, the differences between the models can be detected. APCC model has the lower predictability (represented by red circles) with an annual average of +0.74. The higher correlations are found for both NASA and POAMA models (represented by green and blue circles), with an annual correlation level of +0.92.

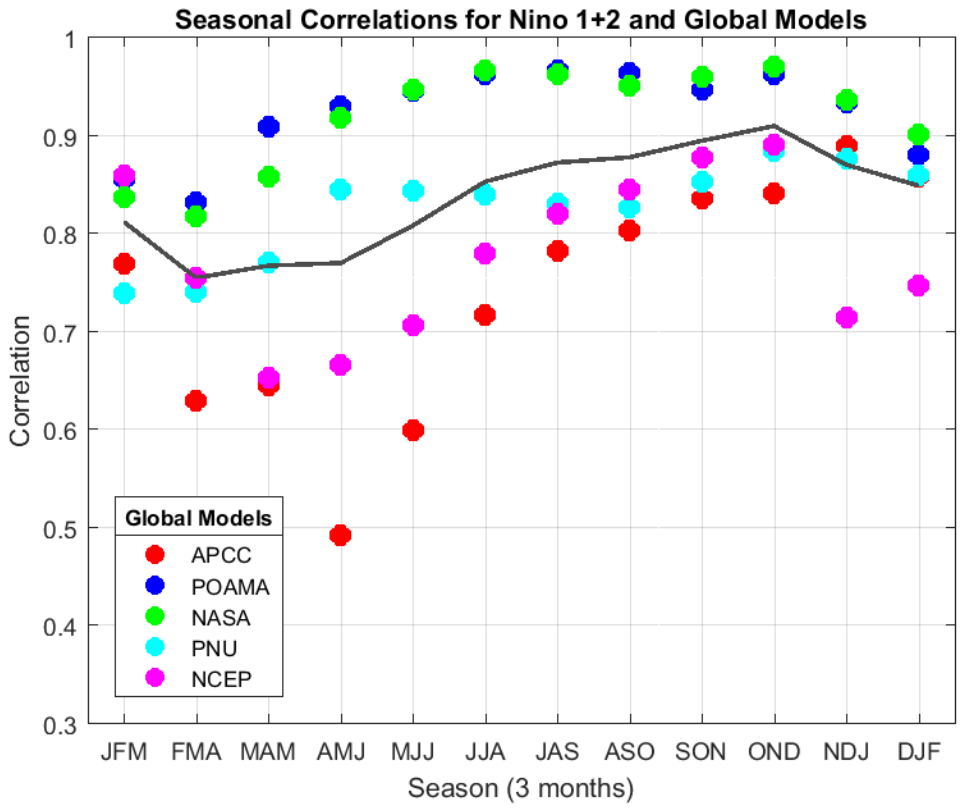

Figure 11. Correlation coefficient for the observed and forecasted El Niño 1+2 index, considering five different models (represented in different colored circles). X-axis represents the quarters of the year. Filled markers represent a 95% or more statistical significance. The gray line corresponds to the average of the five models for every quarter.

3.3. IMPROVEMENTS IN THE CONSTRUCTION OF THE ATMOSPHERIC AND OCEANIC INDICES IN THE MODELS

3.3.1. ATMOSPHERIC INDICES

The extraction process of the monthly values from the data models can be improved if the relationship between the sea surface temperature and sea level pressure were analyzed with the observed indices.

SEP-High represents the intensity of the South East Pacific Subtropical High Pressure. As can be seen in Figure 12, the correlations fields reveal a moderate to high correlation levels facing the coasts of Ecuador, Perú and Northern Chile. The area in front of this region represents the High Pressure intensity rather than the extracted sea level pressures from

eight stations in the coast of Chile. This is why, as can be seen in Figure 12, the second index for SEP-High was created, corresponding to the average sea surface pressure (boxed area) between 250 and 280°E, and within -20°S from the equatorial line.

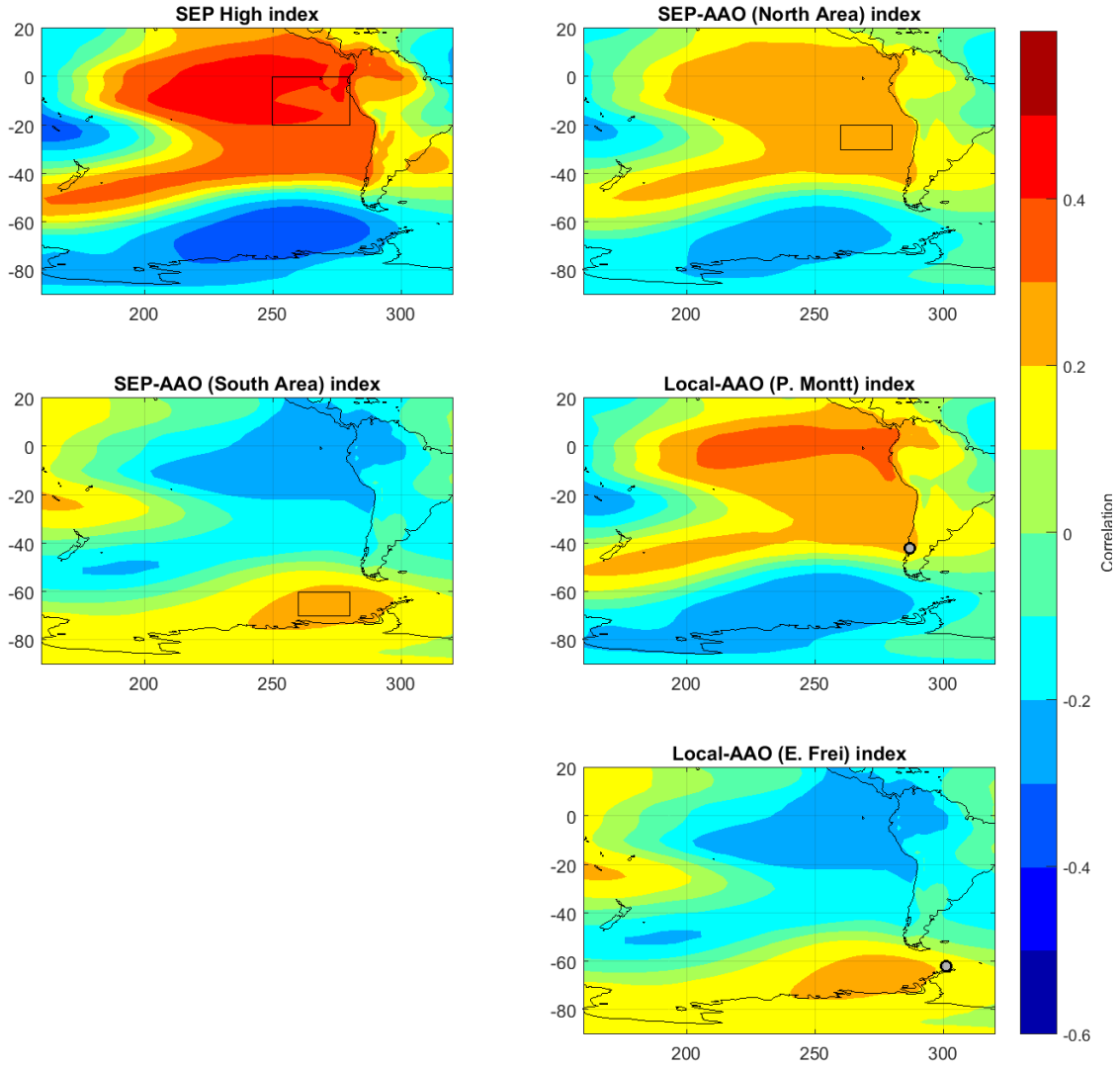

Figure 12. Correlation maps between the averaged (for all months of the year for the five models) sea level pressure field and the SEP-High index; the two areas of the SEP-AAO index and the two points of the Local-AAO index. Solid line represents the new areas where the information for the construction of the indices was extracted.

In the case of the SEP-AAO index, which is the pressure fields difference in two areas of the South Pacific Ocean, both correlations maps in Figure 12 show a low correlation level, with maximum values near +0.3 shifted from the original areas.

A second index was created to represent the SEP-AAO by extracting the average sea level pressure from two new areas in front of Chile; one region located between 20-30°S and 260-280°E, and the other one between 60-70°S and 260-280°E.

In general, it is possible to find an improvement for both SEP-AAO and SEP-High. In the case of the Regional Antarctic Oscillation index, the improvement is very small. This is because it is difficult to find better areas to extract the sea level pressure from the models, which might be due to the models' difficulty of predicting such. For the case of the Anticyclone index, the regular extraction and index construction reach a correlation of +0.48 with the observed index for the whole year. A correlation of +0.59 as the average of the models was computed using the new construction.

3.3.2. OCEANIC INDICES

For all the models with El Niño indices, the sea surface temperature correlation level reveals a high level of direct relation in most of the Tropical Pacific. However, there are some areas with the highest correlation levels representing most of the variability of the El Niño indices. As can be seen in Figure 13, the original construction of the index in the data did not reach the areas with the highest correlation. The solid line represents the original construction and the dotted line, the new indices.

The improvement in the index representation is minimal, but exists. In general, there is an increase in the annual correlation level: from +0.89 to +0.91 for El Niño 4, from +0.92 to +0.93 for El Niño 3.4, from +0.91 to +0.92 for El Niño 3 and from +0.84 to +0.87 for El Niño 1+2.

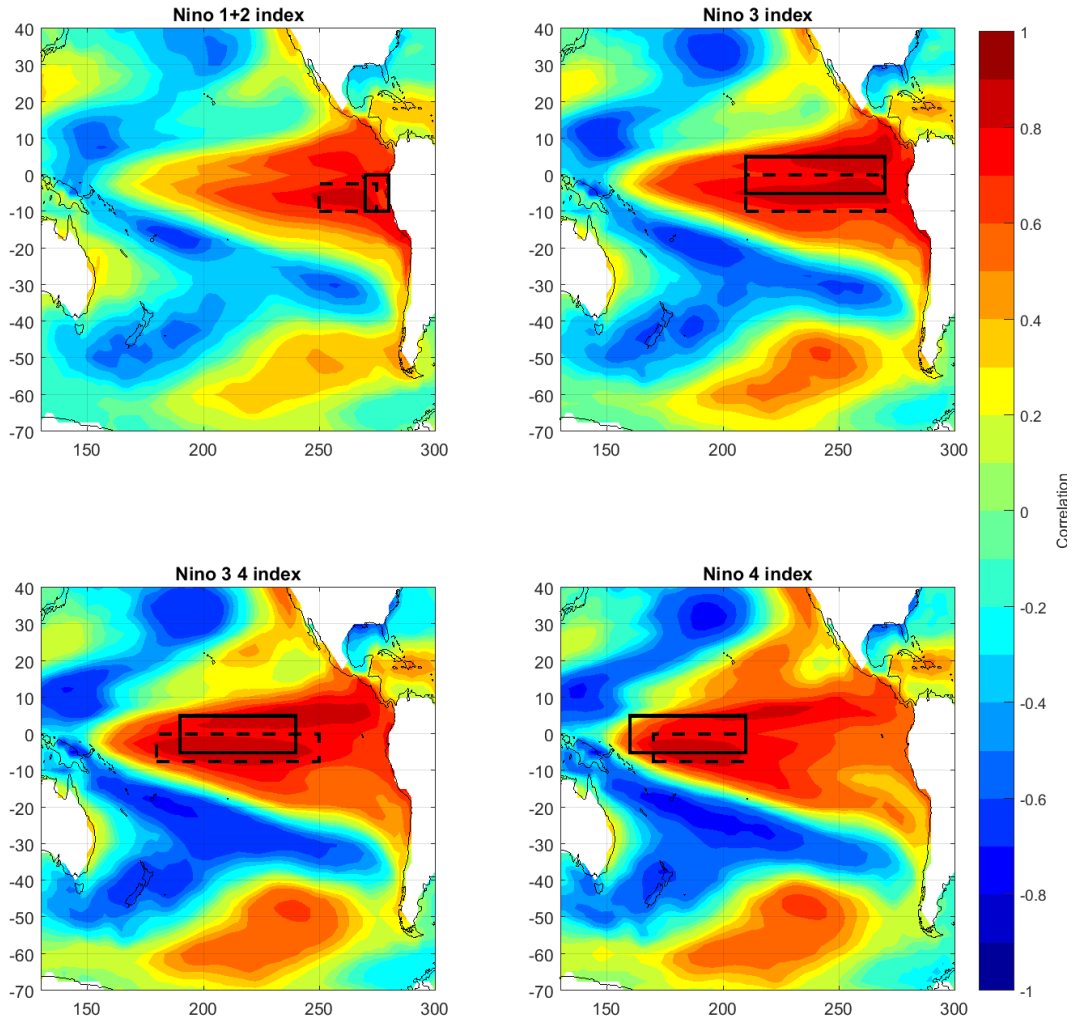

Figure 13. Correlation maps between the averaged (for all the months of the year for the five models) sea surface temperature field and the El Niño indices. The solid line represents the regular areas where the information is extracted for the index construction and the dotted line the new regions for the construction of the new indices.

3.4. PREDICTABILITY OF PRECIPITATION, MAXIMUM TEMPERATURE AND MINIMUM TEMPERATURE FROM THE FORECASTED OCEANIC AND ATMOSPHERIC INDICES

3.4.1. PRECIPITATION

By taking four representative stations, the observed correlation between the quarterly rainfall and the atmospheric and oceanic indices can be compared. Considering the

traditional or normal construction in the models and the new extraction, this can also be compared with the forecasted indices, which was discussed in the previous section.

In the case of SEP-High index, for the stations located in the north and center of the country, similar correlation levels were found in most part of the year, which was improved with the new index. However, the difference between each index is minimal and generates positive bias compared to the expected correlation. Towards the south, the bias becomes more significant. Stations such as Concepción (37°S) or Valdivia (40°S) registered an observed correlation of near -0.6 most of the year. The forecasted indices, both normal and new, did not reach the expected correlation with values near -0.2, except during the spring.

For the SEP-AAO index, same pattern was found. For the stations of La Serena (30°S) and Santiago (33°S), the correlation of normal and new index does not reach the maximum values, especially during winter (JJA and JAS). For Concepción (37°S) and Valdivia (40°S), the correlation is not the same as the observed. During summer, autumn and winter, the correlation is near zero. Similar correlation, however, is found during spring time.

For the case of El Niño indices, similar correlation levels were found compared to the observed, both for the normal and new index. For example, the forecasted indices of La Serena (30°S) and Santiago (33°S) has generated the highest observed correlation levels during the winter and spring with El Niño 3.4. The same happens with El Niño 4, 3 and 1+2.

3.4.2. MAXIMUM TEMPERATURE

For the SEP-High index, the north and central zone had reached the expected correlation level. As can be seen in Figure 14, the new index reached higher inverse correlation compared to the normal index for the Antofagasta station (23°S). This difference becomes lower towards the south. In Valparaíso (33°S), the expected correlation with the new index was only reached during the first quarter of the year. During NDJ and DJF, however, the positive bias is important. During this period, the observed correlation rounds up to -0.6, but the forecasted indices only reach -0.3. For the austral region, Coyhaique (46°S) and Punta Arenas (53°S) reached higher direct correlation during the winter. As can be seen in

Figure 13, the difference is significant between the observed index (black line) and the forecasted indexes (color line). Therefore, it is not possible to reach the highest correlation levels for winter period.

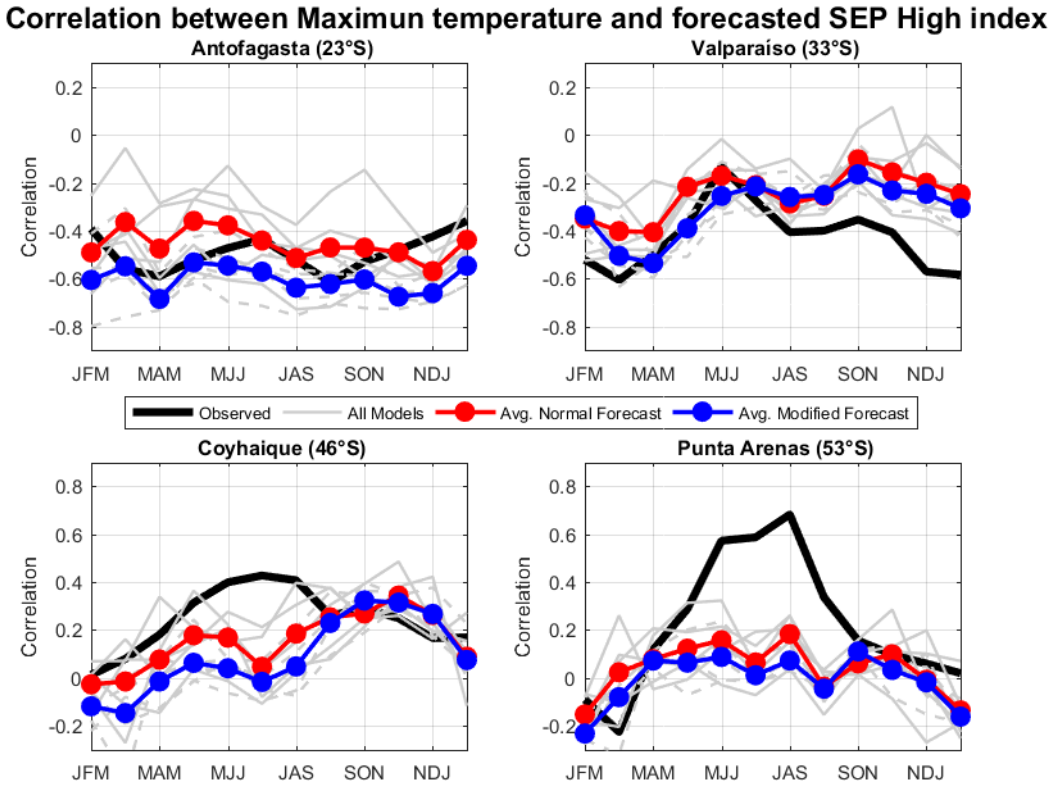

Figure 14. Comparison between SEP-High index and quarterly Maximum Temperature correlations in four stations: Antofagasta (23°S), Valparaíso (33°S), Coyhaique (46°S) and Punta Arenas (53°S). The black line corresponds to the observed correlation. The red and blue lines correspond to the regular and newly extracted index from the average of five global models, respectively. The gray line represents the five different global models used.

For the SEP-AAO index, the forecasted index reaches similar correlation levels to the observed (annual value of r = -0.4). Towards the south, forecasted index did not reach the observed correlation. For example, for Valparaíso station (33°S), the time periods that had the highest observed correlation (r = -0.5) are during the summer, spring and late winter. However, the forecasted index records a Pearson correlation value of about -0.3. In the austral region- Coyhaique (46°S) and Punta Arenas (53°S) stations, the gap between the observed (+0.5) and the forecasted (+0.1) correlation is significant, especially during

winter. It is interesting to notice that there are no major differences between the normal and new index in this correlation.

For the El Niño indices, the forecasted indices is the same as the observed correlation in most of the stations. For example, in Calama (22°S) and Valparaíso (33°S) (Figure 15), the normal and new indices extracted from the models for El Niño 3.4 shows no significant differences with each other. The highest values of correlations with the forecasted indexes are observed for both Calama and Valparaíso. Same behavior was observed for all El Niño regions. With El Niño 1+2, the strong correlation levels are also reached by the indices for the north of the country, with slightly better results with the new index.

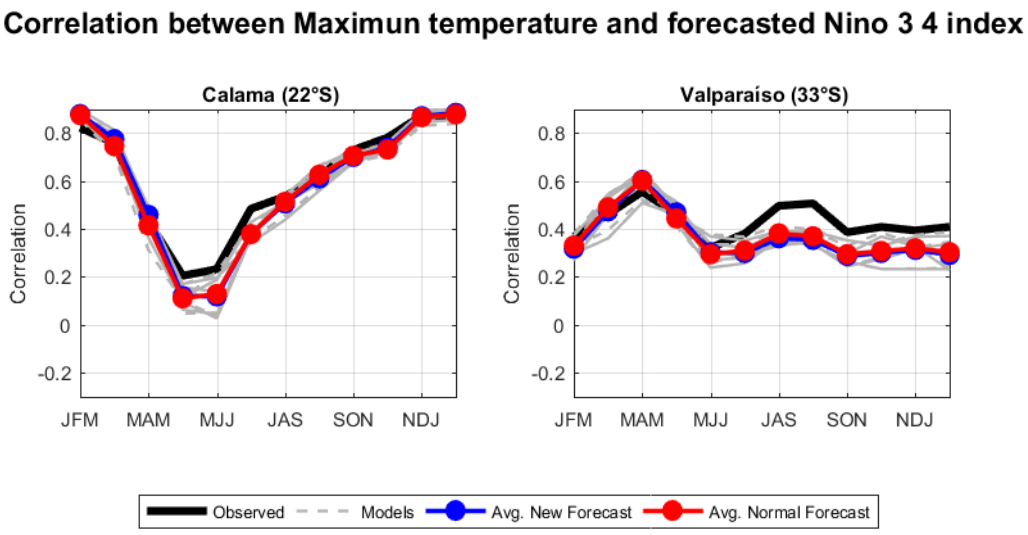

Figure 15. Comparison between the El Niño 3.4 index and quarterly Maximum Temperature correlations in two stations: Calama (22°S) and Antofagasta (33°S). The black line corresponds to the observed correlation. The red and blue lines correspond to the regular and newly extracted index from the average of five global models, respectively. The gray line represents the five different global models used.

3.4.3. MINIMUM TEMPERATURE

Regarding the SEP-High index, the observed correlation is reached by the forecasted indexes for the north of the country. In Antofagasta (23°S) and La Serena (30°S), the new index represents a better approximation of the expected correlation, especially with the new index. In Curicó (35°S) and Concepción (37°S), the observed correlation is around -0.6, but

the forecasted index reaches a correlation level of -0.4 between FMA and SON. In general, correlation results show that there are no significant differences between the new and normal index for these two stations.

With the SEP-AAO index, the observed correlation for both La Serena (30°S) and Antofagasta (23°S) stations have similar values with the forecasted index. Toward the south, the bias is positive and greater. In Curicó (35°S) and Concepción (37°S), the difference between the observed and the forecasted correlation is significant during most part of the year. From MAM to SON, the observed correlation in these cities reach -0.6, but with the forecasted indices, both normal and new, the Pearson correlation is around -0.3.

For all El Niño indices, the correlation results of the forecasted indices are similar to the observed correlation. An example can be seen for the Arica (18°S) and Antofagasta (23°S) stations in Figure 16. The high correlation levels are reached better with the new index, but in general, the difference is minimal.

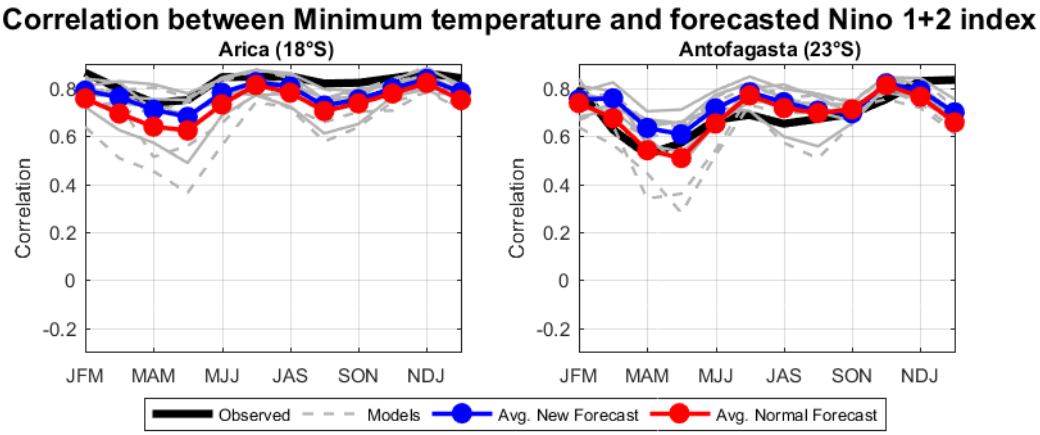

Figure 16. Comparison between the El Niño 1+2 index and quarterly Minimum Temperature correlations for two stations: Arica (18°S) and Antofagasta (23°S). The black line corresponds to the observed correlation. The red and blue line corresponds to the regular and newly extracted index from the average of five global models, respectively. The gray line represents the five different global models used.

4. CONCLUSIONS

This work aims provide an improvement in the seasonal forecast in Chile. The relationship between the different oceanic and atmospheric indices in the rainfall and temperature regimen was analyzed using 40 years-worth of data in 33 stations, covering and distributed throughout most of the country. It is found out that the precipitation and temperature variability in quarters are strongly dependent with the El Niño indices (including El Niño 1+2), which is more evident in the coastal regions. The study also found strong relationship between these variables and the atmospheric indexes of the South East Pacific, such as SEP-High, SEP-AAO and Local-AAO.

For the oceanic indices, corresponding to El Niño 1+2, 3, 3.4 and 4, the five global models used in this study had reached very high levels of predictability. This predictability is higher during the spring and summer. In the case of atmospheric indices, corresponding to SEP-AAO and SEP-High, the predictability is lower compared to the oceanic indices, but still stays within the moderate correlation level.

It was also found out that the indices can be improved, especially El Niño 1+2 and SEP-High, if the construction in the models was changed. In this case, a new way of construction was used without considering the by seasonal differentiation between each model. The forecasted indices can reach the expected correlation levels of the oceanic indices, which will be very useful for seasonal forecast. The forecasted indices had reached the expected atmospheric indices correlation levels only in some regions of the country. This concludes that, in the south and austral region, the forecasted indices are not advisable to be used in practice.

There are no significant differences observed between the normal and new indices, except with SEP-High and El Niño 1+2.

In future works, it is necessary to improve the construction of the indices, both for oceanic and atmospheric, considering the differences between the models and also between seasons. This could help to calculate better indices and reach higher predictability.

6. BIBLIOGRAPHY

Aceituno, P., 1998: On the Functioning of Southern Oscillation in the South American Sector I: Surface Climate. Mon. Wea. Rev.,116: 505-524.

Aceituno, P. and A. Montecinos, 1993: Análisis de la Estabilidad de la Relación de la Oscilación del Sur y la Precipitación en América del Sur. Bulletin de I'nstitute Francais d'Estudes Andines, 22 (1), 53-64.

Garreaud, R. and J. Rutllant, 1996: Análisis Meteorológico de los Aluviones de Antofagasta y Santiago de Chile en el period 1991-1993. ATMÓSFERA (México), 9 (4): 251-271.

Mo, K. C., and R. W. Higgins, 1998: The Pacific-South American Modes and Tropical Convection during the Southern Hemisphere Winter. Mon. Wea. Rev., 126, 1581-1596.

Mo, K. C., 2000: Relationships between Low-Frequency Variability in the Southern Hemisphere and Sea Surface Temperature Anomalies. J. Climate, 13, 3599-3610.

Nan, S., and J. Li, 2003: The relationship between summer precipitation in the Yangtze River valley and the previous Southern Hemisphere Annular Mode. Geophys. Res. Lett., 30(24), 2266.

Rutllant, J., 1987: Synoptic Aspects of the Increase in Rainfall in Central Chile associated with Warm Events in the Central Equatorial Pacific. Proc. Conference on Geophysical Flud Dynamics with special emphasis on El Nino. Sao Jose dos Campos, July 13-17, 1987: 329-342.

Rutllant, J. and H. Fuenzalida, 1991: Synoptic aspectos of the Central Chile rainfall variability associated with the Southern Oscillation. Int. J. of Climatology, 11, 63-76.

Rayner N. A., D. E. Parker, E. B. Horton, C. K. Folland, L. V. Alexander, D. P. Rowell, E. C. Kent, A. Kaplan, Global analyses of sea surface temperature, sea ice, and night marine air temperature since the late nineteenth century, J. Geophys. Res., 108 (D14), 4407, doi:10.1029/2002JD002670, 2003.